Accepted Manuscript

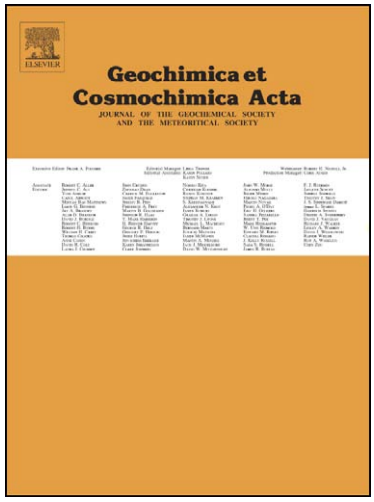

Sorption and catalytic oxidation of Fe(II) at the surface of calcite

Suzanne Mettler, Mariëtte Wolthers, Laurent Charlet, Urs von Gunten

PII: S0016-7037(09)00028-3
DOI: 10.1016/j.gca.2009.01.003
Reference: GCA 5970

To appear in: *Geochimica et Cosmochimica Acta*

Received Date: 12 June 2007
Accepted Date: 13 January 2009

Please cite this article as: Mettler, S., Wolthers, M., Charlet, L., Gunten, U.v., Sorption and catalytic oxidation of Fe(II) at the surface of calcite, *Geochimica et Cosmochimica Acta* (2009), doi: 10.1016/j.gca.2009.01.003

Sorption and catalytic oxidation of Fe(II) at the surface of calcite

Suzanne Mettler[1,4], Mariëtte Wolthers[2,3], Laurent Charlet[2], and Urs von Gunten[1]

[1] Swiss Federal Institute of Aquatic Science and Technology (EAWAG), Ueberlandstrasse 133, 8600 Duebendorf, Switzerland.

[2] Environmental Geochemistry Group, LGIT-OSUG, University of Grenoble, BP 53, F-38041 Grenoble, Cedex 9, France

[3] Department of Earth Sciences - Geochemistry, Faculty of Geosciences, Utrecht University, PO Box 80021, NL-3508 TA Utrecht, The Netherlands.

[4]Address for correspondence:

S. Mettler, Haldenbachstrasse 33, CH-8006 Zürich, Switzerland

Email : suzanne@e-mettler.ch

Phone : +41 79 793 68 66

ABSTRACT

The effect of sorption and coprecipitation of Fe(II) with calcite on the kinetics of Fe(II) oxidation was investigated. The interaction of Fe(II) with calcite was studied experimentally in the absence and presence of oxygen. The sorption of Fe(II) on calcite occurred in two distinguishable steps: (a) a rapid adsorption step (seconds-minutes) was followed by (b) a slower incorporation (hours-weeks). The incorporated Fe(II) could not be remobilized by a strong complexing agent (phenanthroline or ferrozine) but the dissolution of the outmost calcite layers with carbonic acid allowed its recovery. Based on results of the latter dissolution experiments, a stoichiometry of 0.4 mole % Fe:Ca and a mixed carbonate layer thickness of 25 nm (after 168 h equilibration) were estimated. Fe(II) sorption on calcite could be successfully described by a surface adsorption and precipitation model (Comans & Middelburg, *GCA* **51** (1987), 2587) and surface complexation modeling (Van Cappellen et al., *GCA* **57** (1993), 3505; Pokrovsky et al., *Langmuir* **16** (2000), 2677). The surface complex model required the consideration of two adsorbed Fe(II) surface species, $>CO_3Fe^+$ and $>CO_3FeCO_3H^0$. For the formation of the latter species, the stability constant is being suggested. The oxidation kinetics of Fe(II) in the presence of calcite depended on the equilibration time of aqueous Fe(II) with the mineral prior to the introduction of oxygen. If pre-equilibrated for >15 hours, the oxidation kinetics were comparable to a calcite-free system ($t_{1/2}$ = 145 ± 15 min). Conversely, if Fe(II) was added to an aerated calcite suspension, the rate of oxidation was higher than in the absence of calcite ($t_{1/2}$ = 41 ± 1 min and $t_{1/2}$ = 100 ± 15 min, respectively). This catalysis was due the greater reactivity of the adsorbed Fe(II) species, $>CO_3FeCO_3H^0$, for which the species specific rate constant was estimated.

Keywords

Iron, calcite, sorption, surface adsorption and precipitation model, surface complexation model, ferrous iron oxidation, heterogeneous oxidation

1 INTRODUCTION

Iron is the most common metal in sedimentary environments (Cornell and Schwertmann (1996)). The one-electron transfer reaction from the Fe(III) to Fe(II) is associated with an increased Fe availability, because of the much higher solubility of Fe(II) (Stumm and Morgan (1996)). Ground waters with more than 0.3 mg/L ferrous iron should be treated if used for drinking water (0.2 mg/L in the EU: European Communities (1998), WHO (2006), USEPA (2001)), and removal of Fe(II) can be performed by *in-situ* or *ex-situ* techniques. In many *ex-situ* techniques, oxygen or air is bubbled through the ferrous-iron rich ground water (Stumm and Lee (1961), Davison and Seed (1983), Millero et al. (1987), von Gunten and Schneider (1991)). More reducing waters require the addition of stronger oxidants such as chlorine, chlorine dioxide, ozone or permanganate (Knocke et al. (1991), Reckhow et al. (1991), Hoigné and Bader (1994)). Alternatively, Fe(II) removal is often carried out via microbiologically mediated processes (Rundell and Randtke (1987), Mouchet (1992), Benz et al. (1998), Søgaard et al. (2001), Emerson and Weiss (2004)). I*n-situ* ferrous iron removal techniques involve injection of aerated water and the precipitation of Fe oxides (actually, oxyhydroxides and oxides) within the aquifer (Hallberg and Martinell (1976), van Beek (1985), Seyfried and Olthoff (1985), Rott and Meyerhoff (1994), Mettler and von Gunten (2001), Teutsch et al. (2005)). It was shown previously, that *in-situ* removal of iron occurs via surface adsorption, surface oxidation of Fe(II) and precipitation of Fe oxides (Appelo et al. (1999)). This mechanism was found to be responsible for Fe(II) removal at an *in-situ* treatment plant in a calcareous aquifer in north western Switzerland (Mettler and von Gunten (2001), Teutsch et al. (2005)). The present study aims at investigating quantitatively the mechanisms of Fe(II) surface adsorption, precipitation and oxidation in calcite systems.

The speciation of the aqueous Fe(II)-carbonate system has been investigated in dilute solutions by Wersin and collaborators (Charlet et al. (1990), Bruno et al. (1992a), Bruno et al. (1992b), reviewed by King (1998)) as well as in seawater by Millero and co-workers (Millero and Schreiber (1982), Millero and Hawke (1992), Millero (1995), Millero et al. (1995)). In carbonate aquifers, the maximum Fe(II) concentration can either be controlled by the precipitation of siderite, $FeCO_3$(s) (Postma (1981), Wajon et al. (1985), Amirbahman et al. (1998)), or a calcian siderite with 10 mole % Ca^{2+} (Wajon et al. (1985)). Field observations reveal that solid solution continuum between ferroan calcite and calcian siderite is interrupted by a large miscibility gap, where both phases coexist (Reeder (1983)). In laboratory studies, Dromgoole and Walter (1990) determined the homogeneous distribution coefficient for Fe(II) in calcite overgrowths. The maximum Fe concentration they found in calcite at 25°C was < 0.4 mole %. In natural calcite, Fe(II) concentrations range from ~0.68 mole % Fe(II) (marine calcite, Veizer (1983)) to < 3% (fresh water calcite, Di Benedetto et al. (2006), Bolt (2002)).

The kinetics of Fe(II) oxidation by oxygen was investigated in many studies (Stumm and Lee (1961), Singer and Stumm (1970), Davison and Seed (1983), Millero et al. (1987), King (1998), Emmenegger et al. (1998), Rose and Waite (2002), Santana-Casiano et al. (2004)). The reaction kinetics strongly depend on Fe(II) speciation (Luther (1990), Wehrli (1990)). It was shown that aqueous complexation by carbonate ligands catalyzes Fe(II) oxidation in aqueous solutions (King (1998)). Furthermore, it is well established that surfaces act as catalysts for Fe(II) redox reactions but most investigations were carried out on metal oxide surfaces (Tamura et al. (1976), Tamura et al. (1980), Hofstetter et al. (2003), Hiemstra and van Riemsdijk (2007)). The oxidation rate constant was shown to depend on the nature of the oxide (Tamura et al. (1980), Hiemstra and van Riemsdijk (2007)) and the degree of surface complexation (Liger et al. (1999), Silvester et al. (2005)). There is little information available,

however, about the catalytic effect of carbonate surfaces. Loeppert and co-workers (Loeppert and Hossner (1984), Loeppert et al. (1984), Clarke et al. (1985)) have demonstrated that, in the presence of calcite particles, oxidation of Fe(II) is accelerated and increases with the calcite surface concentration.

In this study, adsorption and coprecipitation of Fe(II) on calcite mineral surfaces was investigated experimentally, and results are interpreted and simulated using the surface precipitation models (Comans and Middelburg (1987), Wersin et al. (1989)) and complexation (Van Cappellen et al. (1993), Pokrovsky et al. (2000)). Furthermore, the effect of Fe(II) adsorption and coprecipitation with calcite on the oxidation kinetics was investigated. Experimental kinetics were modelled taking into account the aqueous phase and surface speciation of Fe(II).

2 BACKGROUND: MODELING

2.1 Surface Adsorption and Precipitation Model (SPM)

Comans and Middelburg (1987) used the surface precipitation model originally developed by Farley et al. (1985) for the sorption of cations on metal oxides to describe sorption isotherm data of divalent metal cations on calcite. At low surface coverage, sorption is described as a Langmuir-type monolayer adsorption. At higher surface coverage, the model accounts for the formation of a mixed surface phase, described as a co-precipitated solid solution having as end members the sorbent calcite and a pure carbonate precipitate of the sorbing metal. The model specifies a continuum between adsorption and precipitation, and it was later successfully applied to Mn(II) sorption onto siderite, and supported by spectroscopic information (Wersin et al. (1989)). Table 1 summarizes the reactions, equations and parameters used for the surface precipitation model (Comans and Middelburg (1987), Wersin et al. (1989)). Three independent reactions are involved in the Fe(II)-calcite system, which are described by the reaction constants K_a, K_b and K_c (Table 1, Eqs. 11 to 13): (11) co-precipitation of $FeCO_3(s)$, (12) co-precipitation of $CaCO_3(s)$, as well as (13) the adsorption of Fe(II) onto $CaCO_3(s)$. In the formulation of the surface precipitation model, after adsorption of Fe(II), the calcite surface site, $>CaCO_3^o$, is replaced by the Fe(II) carbonate adsorption site, $>FeCO_3^o$, whereas the original calcium carbonate is incorporated in the bulk solid. Hence, metals at the carbonate/water interface are treated as surface species, whereas metals, which are not in direct contact with the solution, but separated by the adsorption monolayer, are treated as solid species. Surface precipitation leads to the formation of a solid solution, whose composition is described by the distribution coefficient D, defined as the ratio of the precipitation products K_a / K_b. In this model, the precipitation constant (K_a, the inverse of the solubility constant or

$1/K^*_{SO(FeCO3)}$) is an empirical constant, which is corrected by the activity coefficient of the solid species:

$$K_a = \frac{1}{K^*_{so(FeCO_3)} \cdot \bar{\gamma}_{FeCO_3}} \quad \text{(Eq. 1)},$$

with $K^*_{S0(FeCO3)}$, the conditional solubility constant of siderite and $\bar{\gamma}_{FeCO_3}$, the mean activity coefficient of $FeCO_3$ in the co-precipitate, assuming a homogeneous solid solution. K_b is taken as the precipitation constant of calcite ($1/K_{SO(CaCO3)}$), for an infinitely dilute solid solution (i.e. X_{CaCO3} close to one), $\bar{\gamma}_{CaCO_3}$ approaches one. The adsorption constant (K_c) describes the Langmuir-type adsorption of Fe(II) on calcite up to complete saturation of the surface sites, S_T (Table 1). K_a, K_c and S_T depend on each other according to the relation

$$d = \log\left(\frac{K_c S_T}{K_a TotCa}\right) \quad \text{(Eq. 2)},$$

d being the distance between the two asymptotic lines represents the adsorption and the co-precipitation reactions (see *4.5 Modeling Sorption*). The detailed theoretical background of the model and its derivation can be found in Comans and Middelburg (1987) and Wersin et al. (1989). The constants K_a, K_c and the surface site concentration S_T were calculated to best fit the experimental results after transformation of the data according to the equations in Table 1. The best fit was determined from the minimum of the residual sum of squares.

The Vanselow exchange constant, K_{ex}, is often used to describe the affinity of metal cations relative to the calcium ion for the calcite surface (Mc Bride (1980), Zachara et al. (1991), Martin-Garin et al. (2003), Lakshtanov and Stipp (2007)). It can be obtained by division of K_c by K_b (Wersin et al. (1989)):

$K_{ex} = K_c / K_b$ (Eq. 3).

2.2 Surface Complexation Modeling (SCM)

Sorption of divalent cations on carbonate minerals has received ample attention over the last decades. Van Cappellen et al. (1993) proposed a surface complexation model for divalent metal carbonates. Their model is based on acid-base titration data for rhodochrosite ($MnCO_3$) and siderite ($FeCO_3$) and electrophoresis measurements for calcite. Later, their model was refined for calcite (Pokrovsky et al. (2000)) and extended to include other divalent metal carbonates based on ζ-potential and infrared spectroscopy measurements (Cicerone et al. (1992), Pokrovsky et al. (1999a), Pokrovsky et al. (1999c), Brady et al. (1999), Pokrovsky and Schott (2002)). The model postulates the formation of two primary carbonate surface species after hydration, $>MeOH^0$ and $>CO_3H^0$. Other postulated surface species, $>MeOH_2^+$, $>MeO^-$ $>MeHCO_3^0$, $>MeCO_3^-$, $>CO_3Me^+$, $>CO_3^-$ are formed under variable solution conditions. Table 2 summarizes the parameters for the calcite surface reactions and for the Fe(II) speciation.

The software PHREEQC (Parkhurst and Appelo (1999)) was used to calculate the aqueous and surface speciation from thermodynamic data in Table 2. For the calcite surface, no surface charge correction was applied. This is a good approximation since ionic strength effects on the charging behavior of calcite surfaces are insignificant compared to metal oxide surfaces (cf. Van Cappellen et al. (1993)). Note that modeling was performed throughout at calcite saturation, and at the experimental pCO_2 and pH values.

2.2.1 Oxidation Kinetics

It was shown experimentally (Millero et al. (1987), Millero and Izaguirre (1989), Millero et al. (1995), Santana-Casiano et al. (2004)) and by free energy calculations (Luther (1990), Wehrli (1990)) that the pH dependence of the Fe(II) oxidation kinetics is related to Fe(II) speciation

and that each species reacts according to a distinct rate with oxygen. Therefore, in the overall Fe(II) oxidation rate law,

$$-\frac{d[Fe(II)]}{dt} = [O_2]\cdot[Fe(II)]\cdot k_{app} \qquad \text{(Eq. 4)},$$

the apparent rate constant, k_{app}, can be expressed as the sum of the rate constants of each Fe(II) species. King (1998) expanded this model for Fe(II) oxidation by oxygen to carbonate containing solutions:

$$k_{app} = 4(k_1\alpha_{Fe^{2+}} + k_2\alpha_{FeCl^+} + k_3\alpha_{FeSO_4^0} + k_4\alpha_{FeOH^+} + k_5\alpha_{Fe(OH)_2^0} + k_6\alpha_{Fe(HCO_3)^+} +$$

$$k_7\alpha_{Fe(CO_3)^0} + k_8\alpha_{Fe(CO_3)_2^{2-}} + k_9\alpha_{Fe(CO_3)(OH)^-}) \qquad \text{(Eq. 5)}$$

where α is the fraction of each Fe(II) species with respect to the total Fe(II) concentration in solution, and k_i, the second-order rate constants (in $M^{-1}\ s^{-1}$) for the oxidation by oxygen according to reactions (1) to (9) listed in Table 3. The coefficient (4) that appears on the right hand side of equation 5 is the stoichiometric ratio of electrons for the reaction of Fe(II) with oxygen.

In this study, King's model was applied to describe the kinetics of the homogeneous oxidation, that is, Fe(II) oxidation in a solution with no calcite present. The Fe(II) aqueous speciation was calculated in PHREEQC as described above (SCM, Table 2). From the speciation calculation, the values of α for the different aqueous Fe(II) species were calculated. Subsequently, k_{app} was calculated using equation 5 (k_{app} *calculated*) and compared to the experimentally observed k_{app}. The experimental k_{app} was determined by a logarithimic plot of the data according to equation 6, k_{app} being derived by dividing k_{meas}, the first order rate constant, by the oxygen concentration:

$$\ln\frac{[Fe(II)]}{[Fe(II)_0]} = k_{meas}\cdot t, \qquad k_{meas} = k_{app}\times[O_2] \qquad \text{(Eq. 6)}$$

In this study, equation 5 was extended for the calcite containing system to include the Fe(II) surface species and applied to the observed overall heterogeneous oxidation rate data:

$$k_{app} = 4(k_1\alpha_{Fe^{2+}} + k_2\alpha_{FeCl^+} + k_3\alpha_{FeSO_4^0} + k_4\alpha_{FeOH^+} + k_5\alpha_{Fe(OH)_2^0} + k_6\alpha_{Fe(HCO_3)^+} +$$

$$k_7\alpha_{Fe(CO_3)^0} + k_8\alpha_{Fe(CO_3)_2^{2-}} + k_9\alpha_{Fe(CO_3)(OH)^-} + \sum_i^n k_{i,surface-Fe(II)} \cdot \alpha_{i,surface-Fe(II)}) \quad \text{(Eq. 7)}$$

The values of α from the aqueous and surface speciation calculations were again calculated (section 4.6.2). Subsequently, the values of $k_{surface\text{-}Fe(II)}$ were adjusted until k_{app} was in agreement with the experimentally observed k_{app} for 1 g/L and 10 g/L calcite suspensions. For the homogeneous system (no solid), King's values were used (Table 3). There is a strong interdependency between the values for k_6 and k_7 (reactions (6) and (7), Table 3) and no unique solution exists; alternatively maximum values were determined separately by assuming that only one of these species was reactive.

In accordance to King's approach, the ionic strength dependence of k_{app} and k_5 - k_{11} were described by the general form (Millero and Izaguirre (1989)):

$$\log k'_{app} = \log k_{app} + aI^{1/2} + bI \quad \text{(Eq. 8)}$$

where k'_{app} is the apparent Fe(II) oxidation rate constant at an ionic strength I; k_{app} is the Fe(II) oxidation rate constant at I = 0 M; a = –1.338 and b = 0.5747. The rates used in the present study were extrapolated to I = 0 M according to equation 8, they are reported in Table 3.

3 MATERIALS AND METHODS

3.1 Materials

All chemicals used were at least reagent grade. Solutions were prepared with deionized water (Q-H_2O, Barnstead Nanopure). Glassware for the experiments was first cleaned with detergent, then soaked in 10% HNO_3 for at least 12 hours (Stipp and Hochella, (1991)) and rinsed with Nanopure water each time. All oxygen-free experiments with Fe(II) were performed in an anoxic glove box containing a palladium catalyst to remove oxygen (Coy Laboratory Products Inc., Michigan). Fe(II) was added as a stock solution of $FeSO_4 \cdot 7H_2O$ (0.01 M, pH 4; Riedel de Haehn). Fe(II) stock solutions were prepared daily for laboratory experiments and every two days for glove box experiments. Gas mixtures of the desired volume percentage of CO_2 were prepared using proportional flow meters (Brooks Instruments) from pure gases (N_2, CO_2) or gas mixtures (20 % CO_2 in N_2, 8 % O_2 in N_2, and bottled air). $CaCO_3$-saturated water of the desired pH (7.0 ± 0.1) was prepared by equilibrating calcite powder (Merck, Suprapur) and electrolyte (4.1 mM $NaHCO_3$ and 4.9 mM $CaCl_2$) at a CO_2 partial pressure of 3.4 % atm for 4 days. Afterwards, it was filtered and kept under the same CO_2 atmosphere until use. Milling of the calcite crystals and storage of the calcite stock solutions was carried out in $CaCO_3$-saturated water in equilibrium with atmospheric pCO_2 (pH 8.3), but without electrolyte.

3.2 Preparation of the Calcite Suspension

A calcite stock suspension of 1.5-1.8 μm average-sized particles was prepared for this study. Commercially available calcite (Merck, suprapur; mean particle size ca. 80 μm) was milled in suspension in a zircon oxide ball mill. The final concentration of the milled calcite suspension

was 100.7 g L^{-1}, it served as the stock suspension. Size distribution of the particles was measured after the milling procedure and during the experiments by laser diffraction (Malvern Master Sizer X) to verify that grinding by the stir bar did not occur. No measurable changes were observed during the 8 months of experimentation. The specific surface area of the dried solids was 2.4 m^2 g^{-1}, as determined by N_2–BET adsorption.

For the experiments, the stock solution was diluted by addition of $CaCO_3$-saturated water at pH 7 (3.4% atm CO_2) to achieve the desired final $CaCO_3$ concentrations of 1, 2, 10 or 25 g L^{-1}. These suspensions were prepared in sealed glassware at least 4 days before starting the experiments. Within this time, the solution achieved complete equilibrium with the solid. X-ray diffraction analyses revealed no traces of $CaCO_3$ polymorphs (aragonite, vaterite) other than calcite in any of the experimental suspensions within the detection limit of 2 %.

3.3 Analytical Methods

Aqueous Fe(II) was measured with the Ferrozine method on filtered samples (0.2 µm) with a detection limit of 3 x 10^{-7} M in a 1 cm cell (Stookey (1970), Gibbs (1976), Spectrophotometer Uvikon, Bio-Tek Kontron Instruments). The total dissolved Fe concentration was measured spectrophotometrically after reduction of Fe(III) with ascorbic acid. Uncertainty in the determination of Fe was 3% to 5%.

Fe(II) and total Fe concentrations were also determined in the calcite suspensions following calcite dissolution with acetic acid before its quantification with ferrozine. Calibration in the presence of acetic acid was linear over the measured concentration range and showed no interference with acetic acid.

Calcium concentrations of the filtrate from the dissolution experiments (see *Partial Dissolution of the Calcite with CO_2*), were determined on acidified samples (HNO_3, pH 1-2) by inductively coupled plasma atomic emission spectrometry (Spectro; detection limit ≥0.02 mg/L, uncertainty 3%).

Proton concentration was monitored with a pH glass electrode (Orion) calibrated with buffer solutions (Merck, Titrisol; pH 7 and pH 9). Accuracy in pH measurement was 0.05 pH units. Dissolved carbon dioxide concentration at equilibrium with calcite was calculated to yield pH 7.0 and the pCO_2 of the gas mixture was adjusted. A deviation of less than 0.1 pH unit was conceded, equivalent to a maximum deviation in pCO_2 of 8 mbar. The dissolved O_2 concentration was measured with an oxygen sensor (WTW field instrument, Oxi 315i, accuracy ± 0.5% of value, detection limit 1 mg/l).

3.4 Experimental Procedures

All experiments were performed at 20 ± 2°C. They were carried out in batch reactors of various volumes (50-300 cm^3). The desired CO_2 partial pressure in the head space was achieved by sparging the reactor volume with the appropriate bottled gas mixture (carbon dioxide and nitrogen, as well as oxygen for the oxidation experiments). The suspensions were continuously stirred with magnetic stir bars, no milling could be detected by measurement of the particle size distribution.

First, experiments were conducted to study the kinetics, sorption and sorption reversibility of Fe(II) on calcite under oxygen-free conditions. Thereafter, Fe(II) oxidation kinetics in the presence of calcite was investigated by two types of experiments: (1) Addition of Fe(II) to an

aerated calcite suspension, and (2) addition of oxygen after a 15-hour equilibration of Fe(II) with calcite. The experimental data, isotherms and oxidation kinetics, were interpreted using the models presented in the introduction.

3.4.1 Sorption of Fe(II) on Calcite

In the first series of experiments, the sorption kinetics and sorption capacities of Fe(II) on calcite were investigated in an oxygen-free system. For the sorption kinetics experiment, Fe(II) stock solution was added to 250 ml of equilibrated calcite suspensions varying in concentration between 1, 10 and 25 g L^{-1} to achieve a final Fe(II) concentration of 10 µM. Samples (3-4 ml) of the suspension were taken as function of time and the dissolved Fe(II) concentration was measured after filtration (0.2 µm). Adsorption capacities were determined in several batches containing 100 ml of equilibrated calcite suspension (pH 7 ± 0.1; 1 g $L^{-1}$and 2 g L^{-1}). Aliquots of the Fe(II) stock solution were added to achieve total Fe(II) concentrations of 10 to 50 µM, which were equilibrated under constant stirring for 24, 72 or 168 hours. After equilibration, samples were filtered through 0.2 µm nylon filters and the dissolved Fe(II) concentration was determined.

3.4.2 Desorption of Fe(II) with Ligand

Reversibility of the adsorption reaction was examined by addition of the ligands ferrozine or phenantroline to a calcite suspension after it had reacted with Fe(II). Two different ligands were tested to exclude ligand-specific effects with the solid surface. One ml of ferrozine solution (0.02 M) or 2.5 ml of 1, 10-phenanthroline (0.01 M) were added to 50 ml of a calcite suspension (1 g L^{-1}), which had been equilibrated with Fe(II) for 1 h, 5 h, 24 h, 72 h and 168

hours. Samples were taken 1 and 15 hours after ligand addition, filtered (0.2 μm, Nylon) and dissolved Fe(II) was measured.

Recovery of total Fe(II) added to the suspension was also determined to test for possible oxidation of Fe(II). Enough acetic acid was added to the suspension to dissolve the calcite and the resulting solution was analyzed for Fe(II). In general, Fe(II) recovery exceeded 95% of the original concentration. Experiments with smaller recoveries were discarded.

3.4.3 Partial Dissolution of the Calcite with CO_2

The stoichiometry of the Fe(II)-$CaCO_3$ co-precipitates was investigated further by dissolution with carbonic acid. First, Fe(II)-$CaCO_3$ was synthesized in experiments in which calcite (1 g L^{-1}) and 10 μM Fe(II) were equilibrated for 24, 48 or 168 hours. The suspension was then sparged with a gas mixture of either 20% CO_2 (80% N_2, v/v) or 100% CO_2, which partly dissolved the calcite particles until the pH stabilized at 6.5 or 6.0, respectively. Samples were taken regularly over the course of the experiments and analyzed after filtration (0.2 μm) for total dissolved Ca^{2+} and Fe(II).

3.4.4 Fe(II) Oxidation Kinetics in Calcite Suspensions and Control Experiments without Solid

All oxidation experiments were conducted in 100 ml batches of saturated $CaCO_3$ solutions at pH 7. To induce oxidation of Fe(II), bottled air was mixed to the gas flow leading to dissolved oxygen concentrations of either 7.65 (± 0.13) x 10^{-5} M or 2.04 (± 0.16) x 10^{-4} M, which corresponds to thirty times or more the stoichiometric amount needed for oxidation of 10 μM

Fe(II). For the determination of the oxidation rates, data from the lower oxygen concentration (7.65×10^{-5} M) experiments were used.

Fe(II) oxidation kinetics in the presence of calcite were investigated in two ways: (1) by addition of Fe(II) to an aerated calcite suspension, or (2) oxygen was added to a calcite suspension, which had first been equilibrated with Fe(II). In type (1) experiments, Fe(II) was added from a 0.01 M $FeSO_4$ stock solution to achieve a final Fe(II) concentration of 10 µM in an aerated calcite suspension of 1 or 10 g L^{-1}. The suspension was then sampled (3-4 mL) at increasing time intervals. The samples were acidified with an acetic acid/sodium acetate buffer (2 M, final pH of 4.5) to dissolve the calcite and stop the oxidation, filtered and analyzed for Fe(II) immediately. In type (2) experiments, a 1 g L^{-1} calcite suspension was first equilibrated with 10 µM Fe(II) for 15 hours, thereafter, oxidation was started by bubbling the oxygen-containing gas mixture through the suspension. Fe(II) was measured as for type (1) experiments; in addition, at the start of the oxidation, $Fe(II)_{aq}$ was measured in a filtered sample to determine the sorbed fraction of Fe(II).

To account for the effect of the solid phase, control experiments were conducted in homogeneous systems, using solutions that had been equilibrated with calcite and filtered to remove the solid (0.2 µm).

4 RESULTS AND DISCUSSION

4.1 Kinetics

4.1.1 Fe(II) Sorption on Calcite

Figure shows the kinetics of the Fe(II) sorption on calcite for varying solid : solution ratios. Fe(II) adsorption is characterized by a fast initial step (minutes, Fig. 1a) followed by a slow continuous decline, which was measured during a week (168 h) for a calcite concentration of 1 g/L (Fig. 1b).

It was not possible to describe the fast initial decrease of the Fe(II) concentration by a simple rate law. Nevertheless, a minimum first order rate constant for the rapid adsorption step can be estimated from the first data points, which was 2.3 x 10^{-3} s^{-1} at 1 g L^{-1}, 1.15 x 10^{-2} s^{-1} at 10 g L^{-1} and 1.62 x 10^{-2} s^{-1} at 25 g L^{-1} (or 5.7± 3.5 x 10^{-4} L m^{-2} s^{-1}, in average once normalized to the specific surface area of 2.4 m^2/g). The data of the slower stage can be fitted with pseudo-first order kinetics with a slope proportional to the solid: solution ratio. The pseudo first-order rate constants *k'* determined from the slopes were 3.0 x 10^{-6} s^{-1}, 2.8 x 10^{-5} s^{-1} and 7.4 x 10^{-5} s^{-1} for 1, 10 and 25 g L^{-1} calcite, respectively. This corresponds to an average rate constant $k_{sorption}$ of 2.9 ± 0.5 x 10^{-6} L $g^{-1}s^{-1}$ or 1.2 ± 0.1 x 10^{-6} L $m^{-2}s^{-1}$. Therefore, the second phase can be expressed as second order reaction:

$$-d\,[\mathrm{Fe(II)}] / dt = k_{\mathrm{sorption}} \bullet [\mathrm{calcite}] \bullet [\mathrm{Fe(II)}] \qquad \text{(Eq. 9)}$$

The nature of the two sorption stages was further investigated by testing the reversibility of the adsorption. This was done with the two Fe(II) ligands, ferrozine or phenanthroline. In a

first experiment (at 1 g L^{-1} calcite), desorption of Fe(II) with phenanthroline was studied as a function of the equilibration time of Fe(II) with calcite. After 1 hour of equilibration, almost all the sorbed Fe(II) was recovered with phenanthroline. After longer equilibration times of 5, 24 and 72 hours, the irreversibly bound fraction increased, respectively, to 9%, 11% and 21% of the total adsorbed Fe(II) (data not shown). In another experiment, after 168 hours of equilibration of Fe(II) with calcite (at 2 g L^{-1}) at various initial Fe(II) concentrations, between 86% and 94% of the total Fe(II) was irreversibly bound to calcite. Despite the stability of the Fe(II)- ferrozine complex, between 80-90% of the Fe(II) remained associated to calcite even one hour after the ligand addition. The missing Fe(II) could be recovered if calcite was dissolved in acetic acid.

From these results it appears that sorption of Fe(II) on calcite was reversible for equilibration times of up to about 1 hour. After longer equilibration times (> 5 hours), part of the Fe(II) could no longer be recovered by phenanthroline or ferrozine and the fraction of Fe(II) irreversibly bound to calcite increased with equilibration time.

In agreement with these findings, sorption of other transition metals on calcite has been reported to occur in two kinetically distinct stages, a fast initial step (10 to 30 minutes), followed by a slower uptake lasting several days (Lorens (1981), Mn^{2+}: Franklin and Morse (1983); Cd^{2+}: Davis (1987), Martin-Garin et al. (2003); Zn^{2+}: Zachara et al. (1988)). The first step was interpreted as (reversible) adsorption, the second, slower step as incorporation by re-crystallization or co-precipitation. Recrystallization rates are likely affected by the calcite preparation method (Mozeto et al. (1984)).

4.2 Composition of the Fe(II) - Calcite Co - precipitates

The release of Fe(II) induced by dissolution of the calcite by carbonic acid, which had been in contact with Fe(II) for various equilibration times, is presented in Figure 2. During dissolution, both the co-precipitated and the adsorbed Fe(II) were released, such that, depending on the equilibration time, 97% (24 h), 86% (96 h) and 62% (168 h) of the added Fe(II) was recovered. After a 24-hour equilibration period, dissolution with 20% CO_2 led to an almost total recovery of Fe(II), whereas after the longest equilibration time (168 h), approximately 40 % of the total Fe(II) remained associated with calcite.

To get information about the stoichiometry of the dissolved Fe/Ca phase, the released Fe(II) concentrations, $[Fe(II)]_{diss}$, were plotted against the released calcium concentrations, $[Ca^{2+}]_{diss}$. Dissolution data at both CO_2 concentrations (20 % and 100% CO_2) of calcite equilibrated with Fe(II) for 24, 48 and 168 hours are presented in Figure 3. For the 168-hour equilibrated calcite, the amount of Fe(II) and Ca^{2+} released to solution during dissolution are proportional to each other for 0.1 mM < $[Ca^{2+}]_{diss}$ <1 mM. A slope of 0.004 (straight line between 2 mM < Ca^{2+} < 9 mM) was obtained at both CO_2 concentrations and corresponds to the Fe(II)/Ca mole fraction of the Fe(II)-equilibrated calcite over one week (168 h). In other words, calcite of fixed Fe:Ca ratio precipitated upon equilibration with Fe(II). The mole fraction derived from the dissolution experiment coincides with findings of Dromgoole and Walter (1990), who precipitated mixed Fe /Ca carbonates from supersaturated solutions (@ 1 g L^{-1} calcite, pCO_2 0.1-0.97 atm, Ca^{2+} 0.1 mol/l, Fe(II) 0.022 to 0.1 mmol/l) and reported a maximum mole fraction of 0.4 % Fe in the overgrowths formed at the lowest precipitation rate.
At smaller $[Ca^{2+}]_{diss}$ concentrations (< 0.1 mM), the slope is steeper, because it includes also the surface adsorbed Fe(II). Upon further dissolution ($[Ca^{2+}]_{diss}$ > 1 mM), the ratio of

$[Fe(II)]_{diss}$ / $[Ca^{2+}]_{diss}$ gets smaller and this is interpreted as a reduced penetration of Fe(II) into deeper layers of the calcite.

If one assumes that a homogeneous Fe/Ca phase covers the calcite particles of mean grain size 1.8 μm, the thickness of the dissolved layer (Δr) could be roughly estimated from the amount of dissolved calcium. The dissolved layer was estimated to be at most 25 nm and 80 nm, respectively, for the 20 % CO_2 and 100% CO_2 dissolution experiments. The estimated depth to which spherical particles were dissolved appears as a secondary X axis (in nm) in Figure 3. According to theses estimates, the thickness of the mixed Fe / Ca carbonate with the constant mole ratio of 0.4 % after 168 hours of equilibration with Fe(II) would be 25 to 30 nm.

4.3 Fe(II) Oxidation in Presence of Calcite

The oxidation of Fe(II) in the presence of calcite was investigated in two ways to take into account: (i) adsorption and (ii) co-precipitation with the calcite. The main findings are summarized in Figure 4 and Tables 4a and 4b. The decrease of Fe(II) over time could be fitted to pseudo-first order kinetics. A second order rate constant, k_{app}, was then calculated by normalizing to the oxygen concentration. When Fe(II) was added to an oxygen-containing calcite suspension (0.21 mM O_2), it was oxidized faster than in the absence of calcite. The rate constant increased with increasing calcite concentration. Without solid, k_{app} was about 1 $M^{-1}s^{-1}$; at a solid : solution ratio of 1 g/L, k_{app} was close to 2 $M^{-1}s^{-1}$ and at 10 g/L, it was 16 $M^{-1}s^{-1}$. If Fe(II) was equilibrated with calcite for several hours before oxydation, k_{app} was 1 $M^{-1}s^{-1}$ or less, similar to rate constants for the homogeneous solutions.

According to the species dependent rate law proposed by King (1998, equation 5), our results suggest that, in the presence of calcite, a reactive Fe(II) surface complex is formed, which is oxidized faster than the species formed in absence of calcite. However, after longer equilibration times, the Fe(II) surface complex concentration decreased, and its catalytic contribution was no longer noticeable. To further interpret the data, a quantitative description of the surface speciation of Fe(II) on calcite is necessary (see *Modeling Sorption of Fe(II) on Calcite*, 4.5).

4.4 Comparison of Adsorption and Oxidation Kinetics

A comparison of Fe(II) adsorption and oxidation kinetics is shown in Figure. It can be seen that while the rate of adsorption decreased, reflecting a change of the adsorption mechanisms, the oxidation kinetics remained constant over the observation period. Since the presence of $CaCO_3$ accelerated the Fe(II) oxidation, the formation of reactive surface complexes is likely critical and rate-limiting. It was shown above (Figure 5), that during the initial adsorption stage, Fe(II) uptake was described by minimal first-order rate constants of $2 \cdot 10^{-3}$ s^{-1} (1g L^{-1}) and 10^{-2} s^{-1} (10 g L^{-1}), which are significantly higher than the first-order rate constants ($3.8 \cdot 10^{-4}$ $s^{-1}$and $3.4 \cdot 10^{-3}$ s^{-1} for 1 g L^{-1} and 10 g L^{-1}, respectively) of the slow adsorption stage of Fe(II). Since the adsorption of Fe(II) to calcite during the second stage gets significantly slower than the observed oxidation, it can be surmised that the reactive species form during the initial adsorption stage and fast-reacting adsorption sites must be re-generated to maintain the continuously enhanced Fe(II) oxidation. This could be explained by the formation of a new reactive site by Fe(II) oxidation as a result of the production of protons from hydrolysis of Fe(III) and local dissolution of calcite. The formation of Fe(III) hydroxides is more likely than Fe(III) carbonates at the calcite surface. The occurrence of Fe(III) carbonate complex as

well as solid Fe(III) carbonate is scarcely documented. Bolt (2002) reported the presence of Fe(III) hydroxo carbonate in a calcareous lake sediment. Katz et al. (1993) proposed that calcite growth may be inhibited by the formation of a Fe(III) carbonate or hydroxo carbonate complex at the calcite surface. Irrespective, the occurrence of Fe(III) in carbonate environments certainly deserves further investigations by surface specific analyses techniques (AFM, LEED, EXAFS, etc.).

4.5 Modeling Sorption of Fe(II) on Calcite

4.5.1 Surface Adsorption and Precipitation

Three experimental adsorption isotherms were obtained for the 24-hour, 72- or 168-hour equilibration times. The isotherms show a roughly linear behavior for log ΓFe (ΓFe : sorbed Fe(II)) versus log[Fe(aq)]. They can be fitted to a Langmuir isotherm (shown as dotted lines in Figures 6 a - c). Isotherm data were interpreted with the surface precipitation model for divalent metals onto carbonate mineral surfaces (Comans and Middelburg (1987), Wersin et al. (1989)). This model implies a continuum from adsorption to a calcite/siderite solid-solution system. Model parameters and equations are listed in Table 1. As described by equation 20 in Table 1, the sorption density of Fe(II), ΓFe, was normalized with respect to the total calcium concentration (Ca in the calcite and aqueous Ca). Because aqueous calcium was not measured for each point, it was derived from speciation calculations (~2 mM) and added to the amount of calcium in the solid (10 to 20 mM, depending on the calcite concentration). The model requires the adjustment of the total number of sorption sites, S_T, as well as of the adsorption constant, K_c, and of the precipitation constant for siderite as the end member of the $CaCO_3$ – $FeCO_3$ solid solution, K_a. The parameter K_b was taken as the calcite precipitation constant

(inverse of the solubility product as defined by equation 12, Table 1; log K_b = -1.85). Fitting the 24-hour data resulted in a log K_a of -3.60 and log K_c of 0.81 with a surface site concentration S_T of 0.98 site nm^{-2}. Fitting the 72-hour and 168-hour isotherms, assuming the same end member solubility constant (log K_a = -3.60), required a larger sorption constant K_c and a larger surface site concentration than the 24-hour data : logK_c of 1.48 and 2.19, as well as S_T of 1.76 and 2.51 sites nm^{-2} were obtained for 72 hours and 168 hours, respectively. The fits (line) and the data (markers) obtained for the different equilibration times of 24 h, 72 h and 168 h are represented in figures 6a to 6c.

The computed surface site concentrations of 0.98 to 2.51 sites nm^{-2} were similar to values obtained by Comans and Middelburg (1987) for the divalent metals Co, Cd, Mn and Zn (0.11–1.7 sites nm^{-2}). The increasing number of surface sites could be interpreted as evidence of calcite surface modification in response to the co-precipitation of Fe(II). Changes of the surface properties of calcite were reported by Katz et al. (1993) in their calcite growth inhibition studies by Fe(II).

The siderite precipitation constant, defined according to equation 11, (in Table 1) and obtained by fitting of the experimental data (log K_a = -3.60), is close to four orders of magnitude smaller than the value calculated from the siderite solubility constant reported by Preis and Gamsjäger (2002: log $1/K^*_{SO(FeCO3)}$ = + 0.26). It means that Fe(II) is 7270 times less soluble in the calcite lattice than predicted by the thermodynamic solubility constant of siderite. This discrepancy most likely reflects the non-ideality of the $FeCO_3$-$CaCO_3$ solid solution system ($\gamma \approx 7270$, according to Eq.1). Similar results were found by Comans and Middelburg (1987) for the metal (Co, Cd, Mn)- calcite solid solutions: the precipitation constant of the respective end member carbonates were 3 to 5 orders of magnitude smaller than calculated from the

thermodynamic values of the solubility constants (log $1/K^*_{SO}$ of respectively $CoCO_3$(s), $CdCO_3$(s) and $MnCO_3$(s) were -7.0, -4.85 and -4.30).

The mole fraction of $FeCO_3$ in solid solution can be calculated from equation 16 (Table 1). It follows that X_{FeCO3} in the range of 4-5 $x10^{-5}$ is calculated for a calcite solution containing 10^{-5} M Fe(II) (after 24 h equilibration, $[Fe^{2+}]_{aq}$ = 7-8 $x10^{-6}$ M). Using the solubility constant from Preis and Gamsjäger in the same equation would give a X_{FeCO3} between 6 $x10^{-2}$ to 8 $x10^{-2}$. The dissolution experiments yielded a X_{FeCO3} of 4 $x10^{-3}$ (see Composition of the Fe(II)-Calcite Co-precipitates, 4.2).

A comparison of the adsorption constants, K_c, shows that the Fe(II) adsorption constant (log K_c = 0.81 from the 24-hour equilibration) sits between the Cd and Mn values in the sequence of the adsorption constants reported by Comans and Middelburg (1987) for Cd, Mn, Zn and Co (log K_c = 1.43, 0.65, 0.08 and -0.4, respectively). From the adsorption coefficient, an exchange coefficient (K_{ex}) for Fe(II) of $10^{2.66}$ was computed according to Equation 3, which can be compared to values obtained by Zachara et al. (1991) for the divalent cations Cd, Zn, Mn, Co, Ni, Ba and Sr (log K_{ex} of 3.02, 2.43, 1.31, 0.56, 0.51, -1.93 and -2.04, respectively). These were substantiated in later work by Temmam et al. (2000) (Mn and Zn), Hay et al. (2003) and Martin-Garin et al. (2003) (Cd), Lakshtanov and Stipp (2007) (Ni). Accordingly, Fe(II) has only a slightly smaller affinity than Cd. The strong affinity of Fe(II) for the calcite surface compared to the other metal cations Mg, Cd and Sr was confirmed by De Leeuw (2002) based on molecular dynamic simulations: Attachment of $FeCO_3^o$ to calcite step edges was generally more exothermic than for other metal carbonate species both at the acute and obtuse calcite kink sites; a similar result was found for the overgrowth of $FeCO_3$ onto calcite surfaces. Generally, the affinity of the metal cation for the calcite surface seems to be

correlated with the radius of the cation and the solubility product of the respective solid carbonate (Rimstidt et al. (1998), Zachara et al. (1991)). In addition, the coordination geometry of the sorbing metal may play a role. This was demonstrated by Schosseler et al. (1999) for Cu^{2+}, which strongly binds to the carbonate surface by coordination to three surface carbonate ligands in a distorted octahedral configuration. A similar mechanism could explain the strong binding by Fe(II) at the calcite surface and further explain its efficient blocking of reactive sites during calcite growth and dissolution reactions compared to other metal cations (Meyer (1984), Katz et al. (1993), De Leeuw (2002)).

4.5.2 Speciation of Fe(II) on the Calcite Surface

The parameters used in modeling the surface complexation of metal cations such as Mn, Fe or Ca on carbonate minerals were determined in previous studies (Van Cappellen et al. (1993), Pokrovsky et al. (1999a), Pokrovsky et al. (1999b), Pokrovsky et al. (2000); Pokrovsky and Schott (2002); see also Background: Modeling, 2.1and Table 2). None of the present isotherms, however, can be described by the previously postulated Fe(II) surface species, $>CO_3Fe^+$ (Table 2 and Figure 7, dashed line). Adsorption of Fe(II) onto calcite is underestimated.

Co-precipitation of Fe(II) with calcite suggests that Fe(II) is first adsorbed as a carbonate species $FeCO_3^0$, the metal carbonate complex being the building unit of carbonate during crystal growth (De Leeuw (2002)). Adsorption of $FeCO_3^0$ at the calcite surface can be accounted for in the surface complexation model by addition of another reaction. This reaction describes Fe(II) adsorbed as carbonate complex, leading to the Fe species $>CO_3FeCO_3H^0$ (Eq. 10):

$$>CO_3H^0 + FeCO_3 \leftrightarrow >CO_3FeCO_3H^0 \quad \text{(Eq. 10)}$$

The stability constant of Eq. 10 could not be derived from linear combinations of the surface complex reactions of the siderite model (Van Cappellen et al. (1993)). The 24-hour adsorption data (1 and 2 g L-1 calcite) could be well reproduced assuming a log K of 7.4 for the stability constant of Eq. 10. The model results applying SCM and the stabilty constants for $>CO_3Fe^+$ and $>CO_3FeCO_3H^0$ under experimental conditions (total Fe(II) between 10^{-6} and 10^{-4} mol L^{-1}, 4.9 mM $CaCl_2$, 4.1 mM $NaHCO_3$, pH 7.0) is shown in Figure 7. Using the specific surface area of 2.4 m^2/g and the surface site concentration of 5 sites/ nm^2, which represents the number of $>CO_3H^0$ and $>CaOH^0$ at the calcite surface (Möller and Sastri (1974)), the model slightly overestimates the overall uptake of Fe(II) above a concentration of $Fe(II)_{aq}$ $>10^{-5}$ M. The fit could be improved if a smaller value for the surface site concentration of 3 sites /nm^2 was used. Such a discrepancy could indicate that a more complex binding than a 1:1 surface ligand to metal complex is involved. Comparison of the sorption constants show that under the selected experimental conditions, the species $>CO_3FeCO_3H^0$ is more important than $>CO_3Fe^+$.

4.6 Modeling Oxidation Kinetics: Species Specific Rates

4.6.1 Absence of Calcite

King's rate law of the Fe(II) oxidation in carbonate containing solutions was first applied to the experimental data obtained in the calcite-free solution. Speciation calculations were performed to get the fractional composition of the Fe(II) in aqueous solution under the experimental conditions (log pCO_2 -1.75±0.05, pH 7.0 at saturation with calcite, 4.1 mM $NaHCO_3$, 4.9 mM $CaCl_2$, 10 µM $FeSO_4$). Using the rates of King (1998, see Table 3), an

apparent rate constant comparable to the measured value was obtained if maximum values of log k_6 and log k_7 of -2.0 and -3.0, respectively, were used. In this way, a k_{app} of 1.6 to 1.7 $M^{-1}s^{-1}$ was calculated, which is comparable to the experimentally measured k_{app} ranging from 1.3 to 1.8 $M^{-1}s^{-1}$ (see Table 4). In the absence of calcite, the most reactive species were $Fe(CO_3)_2^{2-}$, $Fe(OH)_2$, $Fe(CO_3)(OH)^-$ and $Fe(OH)^+$ which contributed, respectively, 72%, 15%, 12% and 2% of the overall apparent rate constant. The same order of reactivity was observed in King's system with respective contributions to the overall rate of 50%, 27%, 19% and 3% (King (1998)). In King's system, the total carbonate concentration (ΣCO_2, HCO_3^- CO_3^{2-}) increased with pH. In our system, the ΣCO_2 is controlled by calcite solubility and, thus, increases as pH decreases (see also below, Figure 8).

4.6.2 Reactive Fe(II)-Calcite Surface Species.

Oxidation of Fe(II) was faster in the presence of calcite than in a homogeneous calcite-free solution but if calcite was first equilibrated with Fe(II) before oxidation, no catalysis was observed. The faster oxidation of Fe(II) in the presence of calcite was interpreted as a higher reactivity of the adsorbed species. By analogy to the reactivity of the aqueous species, the species $>CO_3FeCO_3H^0$ must be more reactive than $>CO_3Fe^+$ because, under homogeneous conditions (i.e., in the absence of calcite), $Fe(CO_3)_2^{2-}$ is oxidized faster than the carbonate species $FeCO_3^0$ and $FeHCO_3^0$. In addition, the same surface species, $>CO_3FeCO_3H^0$, is expected to be involved in the co-precipitation reaction as it is the most probable precursor of a Fe(II)-Ca carbonate phase at the calcite surface (De Leeuw (2002)). Co-precipitation was shown to occur in the sorption experiments, if calcite and Fe(II) were equilibrated for several hours in the absence of oxygen. A later oxidation of the equilibrated suspension did not show any acceleration of the Fe(II) oxidation. The sorbed Fe(II) seemed to be physically protected

and no longer available to the oxidant. Therefore, after extended pre-equilibration with calcite, only the aqueous Fe(II) was oxidized and the overall oxidation rate was equivalent to the calcite-free system.

Based on these considerations, a species specific oxidation rate constant was determined for the fast reacting species, $>CO_3FeCO_3H^0$, using the experimental data obtained at 1 g L^{-1} and 10 g L^{-1} and speciation calculations including the Fe(II) surface species of the SCM described in Table 2 and Figure 7. The resulting Fe(II) speciation in a 1 g L^{-1} calcite suspension is illustrated in Figure 8. The adsorbed species $>CO_3FeCO_3H^0$ represents 25% of the total Fe(II) at 1 g L^{-1} calcite and 79 % at 10 g L^{-1}. Given the speciation established above, the best fit to the measured apparent second order rate constant was obtained with a species specific rate constant for $>CO_3FeCO_3H^0$ of 2.5 $M^{-1}s^{-1}$. This resulted in calculated apparent rate constants, $k_{app,calc}$ of 3.8 $M^{-1}s^{-1}$ and 8.2 $M^{-1}s^{-1}$ at 1 g L^{-1} and 10 g L^{-1} calcite, respectively. This predicts the measured rate constant at 1 g L^{-1} well (the measured $k_{app,}$ was 2 to 3.8 $M^{-1}s^{-1}$), but it underestimates the rate constant at 10 g L^{-1} by a factor of nearly two (the measured $k_{app,}$ was 15.8 $M^{-1}s^{-1}$; see Table 4). The fit is improved if a species rate constant of 5 $M^{-1}s^{-1}$ is assumed. This yields an overall rate constant of 16 $M^{-1}s^{-1}$ at 10 g L^{-1} calcite and of 6.2 $M^{-1}s^{-1}$ at 1 g L^{-1} calcite. Therefore, the species specific rate constant, $k_{>CO3FeCO3H,}$ ranges between 2.5 and 5 $M^{-1}s^{-1}$ (or $0.4 > log\ k_{>CO3FeCO3H} > 0.7$ $M^{-1}s^{-1}$). Correction for the ionic strength effect according to Equation 8 results in a rate constant $log\ k_{>CO3FeCO3H}$ at I= 0 M of 0.72 ± 0.15 $M^{-1}s^{-1}$. Using the species specific rate constants of Table 3 and results of the speciation calculation, the relative contribution of the different Fe(II) species to the overall rate constant can be calculated (Figure 9.) At a calcite concentration >1 g L^{-1}, the adsorbed Fe(II) species has the highest contribution to Fe(II) oxidation, followed by the species $Fe(CO_3)_2^{2-}$ > $Fe(OH)_2$

> $Fe(CO_3)(OH)^-$. The contribution of the surface species increases to over 80% of the total oxidation rate at a calcite suspension concentration of >2 g L^{-1}.

Similarly, calculated and measured apparent rate constants k_{app}, can be compared for the case where Fe(II) was equilibrated with calcite several hours before oxygen addition. Results are shown in Table 4b. This time, it was assumed that the species $>CO_3FeCO_3H^0$ was not present, because incorporated as a $Fe/CaCO_3$ co-precipitate in the bulk solid. Model calculations yielded apparent rate constants at a concentration of 1 g L^{-1} calcite, $k_{app,calc}$, in the range of 1.1 to 1.4 M^{-1} s^{-1} (6.95 < pH < 7.06). This is in agreement with the measured apparent rate constants, k_{app} , of 0.6 to 1.1 M^{-1} s^{-1} obtained after 15 to 24-hour pre-equilibration. After longer pre-equilibration times of 72 to 168 hours (1 week), smaller apparent rate constants were measured (0.2 M^{-1} s^{-1} < k_{app} < 0.7 M^{-1} s^{-1}). Variations of apparent rate constant with pre-equilibration times are consistent with the progressive co-precipitation of the Fe(II).

4.6.3 Importance of the calcite-promoted Fe(II) oxidation in the natural environment.

With the parameters of Tables 2 and 3, the contribution of the reactive Fe(II) species to the overall Fe(II) oxidation rate as function of the pH can be calculated. This is shown in Figure 10 for a calcite-saturated suspension of 1 g/L, 10^{-5} M $FeSO_4$, a set background salt concentration (4.1 mM $NaHCO_3$, 4.9 mM $CaCl_2$) and variable pH. According to Figure 10, the surface species $>CO_3FeCO_3H^0$ is the most reactive species below pH 7.5, followed by $Fe(CO_3)_2^{2-}$. Above pH 7.5, the hydroxo-species $Fe(OH)_2$ becomes more important and even rate controlling above pH 8. The importance of the adsorbed Fe(II) species, which is dominant below pH 7 (see Figure 8), should be further investigated to confirm these predictions. At high

calcite and low oxygen concentrations, Fe(II) could be rapidly co-precipitated and its oxidation efficiently inhibited.

5 CONCLUSIONS

The sorption behavior of Fe(II) in a calcite-water system was investigated in the absence of oxygen. The results showed that Fe(II) binds to calcite (i) by surface adsorption and (ii) by co-precipitation forming a mixed Fe/Ca carbonate phase. Co-precipitation kinetics of Fe(II) into calcite could be fitted to first order kinetics with respect to the solid concentration. Incorporation was clearly detected in sorption experiments conducted for more than 15 hours. After this time, it was not possible to recover all of the added Fe(II) using strong Fe(II) ligands, such as ferrozine or phenanthroline, contrasting to the results of shorter equilibration time. Dissolution of the Fe(II)-equilibrated calcite with carbonic acid allowed complete recovery of the Fe(II) revealing that a ferrous calcite solid solution had formed with a Fe(II) to calcium molar ratio close to 0.4 %.

Sorption isotherms measured at pH 7 with 1 or 2 g/L calcite after more than 24 hours displayed two uptake mechanisms for Fe(II) sorption on calcite: (i) Langmuir-type adsorption at low metal coverage and (ii) co-precipitation at high metal surface concentrations. The adsorption-precipitation model previously used by Comans and Middelburg (1987) to simulate sorption of Mn, Cd, and Co to calcite successfully described our data. In contrast, a straightforward surface complexation model describing sorption of Fe(II) to a single adsorption site $>CO_3Fe^+$ could not reproduce the isotherm data. Consideration of the additional surface reaction, $>CO_3H^0 + FeCO_3^0 = >CO_3FeCO_3H^0$, with a log K of 7.4 was necessary. The nature of ferrous complexes at the calcite surface has not yet been confirmed by spectroscopic methods but we propose that the adsorbed ferrous carbonate species $>CO_3FeCO_3H^0$ is a likely precursor in the formation of the $Fe/CaCO_3$ surface precipitate (De

Leeuw (2002)), which forms after a long exposure of dissolved Fe(II) to calcite under anaerobic conditions.

Finally, the effect of oxygen addition on the Fe(II) - calcite system was investigated. The presence of calcite accelerated Fe(II) oxidation relative to an equivalent calcite-free system. Based on a surface complexation model, and in analogy to the study by King (1998) about the acceleration of the Fe(II) oxidation by carbonate species (in particular by the species $Fe(CO_3)_2^{2-}$), the species-specific oxidation rate constant for the surface species $>CO_3FeCO_3H^0$ was determined, $log\ k_{>CO3FeCO3H} = 0.72 \pm 0.15\ M^{-1}s^{-1}$ at I=0. However, if Fe(II) and calcite were equilibrated several hours before exposure to oxygen, the measured oxidation rate constant was lower than in the absence of calcite. We propose that Fe(II) is progressively incorporated in the calcite lattice, where it is no longer susceptible to oxidation. In both cases, the measured oxidation rate constants could be reproduced by speciation and kinetics calculations.

ACKNOWLEDGMENTS

The author thanks Stephan Hug and Denis Mavrocordatos† for fruitful advice thoughout the experimental studies. Paul Wersin is acknowledged for his continuing support. Lisa Salhi and Hansjuergen Schindler provided technical assistance. S. M. acknowledges funding by KTI. L.C. acknowledges partial funding of this research by RECOSY and by the ANR Geocarbone-Carbonation, and M. W. partial funding by ANDRA and VENI grant #016.071.018 of NWO. The authors also thank the associate editor and the three anonymous reviewers for their helpful comments.

REFERENCES

Amirbahman A., Schoenenberger R., Johnson C. A. and Sigg L. (1998) Aqueous- and solid-phase biogeochemistry of a calcareous aquifer system downgradient from a municipal solid waste landfill (Winterthur, Switzerland). *Environ. Sci. Technol*. **32**, 1933-1940.

Appelo C. A. J., Drijver A., Hekkenberg R. and de Jonge M. (1999) Modeling in situ iron removal from ground water. *Ground Water* **6** (37), 811-816.

Benz M., Brune A., Schink B. (1998) Anaerobic and aerobic oxidation of ferrous iron at neutral pH by chemoheterotrophic nitrate-reducing bacteria. *Arch. Microbiol*. **169**, 159-165.

Bolt M. (2002) Iron sulfides in Baldeggersee during the last 8000 years: formation processes, chemical speciation and mineralogical constraints from EXAFS spectroscopy, Ph.D. Thesis, ETH-Zürich, 104 pp.

Brady P. V., Papenguth H. W. and Kelly J. W. (1999) Metal sorption to dolomite surfaces. *Appl. Geochem.* **14** (4) 569-579.

Bruno J., Stumm W., Wersin P. and Brandberg F. (1992a). On the influence of carbonate in mineral dissolution: I. The thermodynamics and kinetics of hematite dissolution in bicarbonate solutions at 25°C. *Geochim. Cosmochim. Acta* **56** (3), 129-1147.

Bruno J., Wersin P. and Stumm W. (1992b). On the influence of carbonate in mineral dissolution: II. The solubility of $FeCO_3$ (s) at 25°C and 1 atm total pressure. *Geochim. Cosmochim. Acta* **56** (3), 1149-1155.

Charlet L., Wersin P. and Stumm, W. (1990). Surface charge of $MnCO_3$ and $FeCO_3$. *Geochim. Cosmochim. Acta* **54** (8), 2329-2336.

Cicerone D.S., Regazzoni A. E. and Blesa M.A. (1992). Electrokinetic properties of the calcite/water interface in the presence of magnesium and organic matter. *J. Colloid Interface Sci.* **154** (2), 423-433.

Clarke E. T., Loeppert R. H. and Ehrman J. M. (1985) Crystallization of iron oxides on calcite surfaces in static systems. *Clays Clay Min*. **33** (2).

Comans R. N. J. and Middelburg J. J. (1987). Sorption of trace metals on calcite: Applicability of the surface precipitation model. *Geochim. Cosmochim. Acta* **51** (9), 2587-2591.

Cornell R. M. and Schwertmann U. (1996) *The iron oxides. Structure, properties, reactions, occurence and uses.* VCH, Weinheim.

Davis J.A., Fuller C. C. and Cook A. D. (1987) A model for trace metal sorption processes at the calcite surface: adsorption of Cd^{2+} and subsequent solid solution formation. *Geochim. et Cosmochim. Acta* **51** (6), 1477-1490.

Davison W. and Seed G. (1983) The kinetics of the oxidation of ferrous iron in synthetic and natural waters. *Geochim. Cosmochim. Acta* **47** (1), 67-69.

De Leeuw N. H. (2002) Molecular dynamics simulations of the growth inhibiting effect of Fe^{2+}, Mg^{2+}, Cd^{2+}, and Sr^{2+} on calcite crystal growth. *J. Phys. Chem. B* **106***,* 5241-5249.

Di Benedetto F., Costagliola P., Benvenuti M., Lattanzi P., Romanelli M. and Tanelli G. (2006) Arsenic incorporation in natural calcite lattice: Evidence from electron spin echo spectroscopy, *Earth Planet. Sci. Letters* **246**, 458–465.

Dromgoole E. L. and Walter L. M. (1990) Iron and manganese incorporation into calcite: effect of growth kinetics, temperature and solution chemistry. *Chem. Geol.* **81**, 311-336.

Emerson D. and Weiss J. V. (2004) Bacterial iron oxidation in circumneutral freshwater habitats: findings from the field and the laboratory. *Geomicrobiol. J.* **21** (6), 405-414.

Emmenegger L., King D. W., Sigg L. and Sulzberger B. (1998) Oxidation kinetics of Fe(II) in an eutrophic Swiss lake. *Environ. Sci. Technol*. **32**, 2990-2996.

European Communities (1998). Drinking Water Directive; Council Directive 98/83/EC. *Official Journal of the European Communities* L330/32 from 5.12.1998. (http://eur-lex.europa.eu/LexUriServ/site/en/oj/1998/l_330/l_33019981205en00320054.pdf).

Farley K. J., Dzombak D. A. and Morel F. M. (1985). A surface precipitation model for the sorption of cations on metal oxides. *J. Colloid Interface Sci.* **106** (1), 226-242.

Franklin M. L. and Morse J. W. (1983) The interaction of manganese(II) with the surface of calcite in dilute solutions and seawater. *Marine. Chem*. **12**, 241-254.

Gibbs C. R. (1976) Characterization and application of Ferrozine iron reagent as a ferrous iron indicator. *Analytical Chemistry*. **48** (8, July), 1197-1201.

Hallberg R. O. and Martinell R. (1976) Vyredox - In situ purification of ground water. *Ground Water.* **14** (2), 88-93.

Hay M. B., Workman R. K. and Manne S. (2003). Mechanisms of metal ion sorption on calcite: composition mapping by lateral force microscopy. *Langmuir*. **19**, 3727-3740.

Hiemstra T. and van Riemsdijk W. H. (2007) Adsorption and surface oxidation of Fe(II) on metal (hydr)oxides . *Geochim. Cosmochim. Acta*. **71** (7), 5913-5933.

Hofstetter T. B., Schwarzenbach R. P., and Haderlein S. B. (2003) Reactivity of Fe(II) species associated with clay minerals. *Environ. Sci. Technol*. **37**, 519–528.

Hoigné J. and Bader H. (1994). Kinetics of reaction of chlorine dioxide (OClO) in water - I: Rate constants for inorganic and organic compounds. *Wat. Res.* **28** (1), 45-55.

Katz J. L, Reick M. R., and Parsiegla K. I. (1993) Calcite growth inhibition by iron. *Langmuir* **9** (5), 1423-1430.

King D. W. (1998) Role of carbonate speciation on the oxidation rate of Fe(II) in aquatic systems. *Environ. Sci. Technol.* **32**, 2997-3003.

Knocke W. R., Benschoten J. E. V., Kearney M. J., Soborski A. W. and Reckhow D. A. 1991). Kinetics of manganese and iron oxidation by potassium permanganate and chlorine dioxide. *J. Am. Wat. Work. Ass.* **83** (6), 80-87.

Kostka J. E. and Luther III G. W. (1994) Partitioning and speciation of solid phase iron in saltmarsh sediments. *Geochim. Cosmochim. Acta*. **58** (7), 1701-1710.

Lakshtanov L.Z. and Stipp S.L.S (2007) Experimental study of nickel(II) interaction with calcite: Adsorption and coprecipitation. *Geochim. Cosmochim. Acta*. **71** (15), 3686-3697.

Liger E., Charlet L. and Van Cappellen P. (1999) Surface catalysis of uranium (VI) reduction by iron(II). *Geochim. Cosmochim. Acta* **19** (20), 2939-2956.

Loeppert R. H. and Hossner L. R. (1984) Reactions of Fe^{2+} and Fe^{3+} with calcite. *Clays Clay Min*. **32** (3), 213-222.

Loeppert R. H., Hossner L. R. and Amin P. K. (1984) Formation of ferric oxyhydroxides from ferrous and ferric perchlorate. *Soil Sci. Soc. Am. J.* **48**, 677-683.

Lorens R. B. (1981) Sr, Cd, Mn and Co distribution coefficient in calcite as a function of calcite precipitation rate. *Geochim. Cosmochim. Acta*. **45** (4), 553-561.

Luther III G. W. (1990) The frontier-molecular-orbital theory approach in geochemical processes. *Aquatic chemical kinetics* (ed. W. Stumm), pp. 173-198. John Wiley & Sons, Inc. New York.

Martin-Garin A., Van Capellen P. and Charlet L. (2003) Aqueous cadmium uptake by calcite: A stirred flow-through reactor study. *Geochim. Cosmochim. Acta* **67** (15), 2763-2774.

Mc Bride M. B. (1980) Chemisorption of Cd^{2+} on calcite surfaces. *Soil Sci. Soc. Amer. J.* **44**, 26-28.

Mettler S. and von Gunten U. (2001) Characterization of iron and manganese precipitates from an in situ ground water treatment plant. *Ground Water* **39** (6), 921-930.

Meyer H. J. (1984). The influence of impurities on the growth rate of calcite. *J. of Crystal Growth* **66**, 639-646.

Millero F. J. (1995) Thermodynamics of the carbon dioxide system in the oceans. *Geochim. Cosmochim. Acta* **59** (4), 661-677.

Millero F. J. and Hawke D. J. (1992) Ionic interactions of divalent metals in natural waters. *Marine Chem.* **40**, 19-48.

Millero F. J. and Izaguirre M. J. (1989) Effect of ionic strength and ionic interactions on the oxidation of Fe(II) *J. Solution Chem.* **18**, 585-599.

Millero F. J. and Schreiber D. R. (1982) Use of the ion pairing model to estimate the activity coefficient of the ionic components of natural waters. *Am. J. Sci.* **282**, 1508-1540.

Millero F. J., Sotolongo S. and Izaguirre M. (1987) The oxidation kinetics of Fe(II) in seawater. *Geochim. Cosmochim. Acta* **51** (4), 793-801.

Millero F. J., Yao W. and Archer J. (1995) The speciation of Fe(II) and Fe(III) in natural waters. *Marine Chem.* **50**, 21-39

Mouchet P. (1992) From conventional to biological removal of iron and manganese in France. *J. Am. Water Works Assoc.* **April**, 158-167.

Mozeto A. A., Fritz P. and Reardon E. J. (1984) Experimental observation on carbon isotope exchange in carbonate-water systems. *Geochim. Cosmochim. Acta* **48** (3), 495-504.

Möller P. and Sastri C. S. (1974) Estimation of the number of surface layers of calcite involved in ^{45}Ca-Ca isotopic exchange with solution. *Z. Phys. K. Chem. Folge* **89**, 80-87.

Parkhurst D.L. and Appelo C.A.J. (1999) User's guide to PHREEQC (vers.2) – a computer program for speciation, batch reaction, one-dimensional transport and inverse geochemical calculations. *U.S.G.S. Water resource Invest. Report* 99/4259, 312p.

Pitzer K. S. (1991) Ion interaction approach: Theory and data correlation. *Activity coefficients in electrolyte solutions* (ed.: Pitzer K.S.). CRC Press, Boca Raton, FL. pp. 75-153.

Plummer L. N. and Busenberg E. (1982) The solubilities of calcite, aragonite and vaterite in CO_2-H_2O solutions between 0 and 90°C, and an evaluation of the aqueous model for the system $CaCO_3$-CO_2-H_2O. *Geochim. Cosmochim. Acta* **46** (11)**,** 1011-1040.

Pokrovsky O. S., Mielczarski J. A., Barres O. and Schott J. (2000) Surface speciation models of calcite and dolomite/aqueous solution interfaces and their spectroscopic evaluation. *Langmuir* **16** (6), 2677-2688.

Pokrovsky O. S. and Schott J. (2002) Surface chemistry and dissolution kinetics of divalent metal carbonates. *Environ. Sci. Technol*. **36**, 426-432.

Pokrovsky O. S., Schott J. and Thomas F. (1999a) Processes at the magnesium-bearing carbonates/solution interface. I. A surface speciation model for magnesite. *Geochim. Cosmochim. Acta* **63** (6), 863-880.

Pokrovsky O. S. and Schott J. (1999b) Processes at the magnesium-bearing carbonates/solution interface. II. kinetics and mechanism of magnesite dissolution. *Geochim. Cosmochim. Acta* **63** (6), 881-897.

Pokrovsky O. S., Schott J. and Thomas F. (1999c) Dolomite surface speciation and reactivity in aquatic systems. *Geochim. Cosmochim. Acta.* **63** (19-20), 3133-3143.

Postma D. (1981) Formation of siderite and vivianite and the porewater composition of a recent bog sediment in Denmark. *Chem. Geol*. **31**, 225-244.

Preis W. and Gamsjäger H. (2002) Critical evaluation of solubility data: enthalpy of formation of siderite. *Phys. Chem. Chem. Phys.* **4**, 4014-4019.

Reckhow D. A., Knocke W. R. and Kearney M. J. (1991) Oxidation of iron and manganese by ozone. *Ozone Sci and Eng.* ***13*****,** 675-695.

Reeder R. R. (1983) Carbonates: Mineralogy and Chemistry. In *Reviews in Mineralogy*, Vol. 11. Mineralogical Society of America, Washington D.C.

Rimstidt D., Balog A. and Webb J. (1998) Distribution of trace elements between carbonate minerals an aqueous solutions. *Geochim. Cosmochim. Acta* **62** (11), 1851-1863.

Rose A. and Waite T. D. (2002) Kinetic model for Fe(II) oxidation in seawater in the absence and presence of natural organic matter. *Environ. Sci. Technol. 36, 433-444.*

Rott U. and Meyerhoff R. (1994) Physical, chemical and biological processes in consequence of in-situ treatment of groundwater. Proceedings of the Groundwater Quality Management Conference, Tallinn, 1993; pp. 439-447.

Rundell B. D. and Randtke S. J. (1987) In situ ground water treatment for iron and manganese: fundamental, practical, and economic considerations. Annual Conference American Water Works Association. Kansas City, MO, 513-533.

Santana-Casiano J. M., Gonzalez-Davila M. and Millero F. J. (2004) The oxidation of Fe(II) in NaCl – HCO_3^- and seawater solutions in the presence of phthalate and salicylate ions: a kinetic model. *Marine Chem*., **85**, 27-40.

Schosseler P. M., Wehrli B. and Schweiger A. (1999) Uptake of Cu^{2+} by the calcium carbonates vaterite and calcite as studied by continuous wave (CW) and pulse electron paramagnetic resonance. *Geochim. Cosmochim. Acta* **63** (13/14), 1955-1967.

Seyfried C. F. and Olthoff R. (1985) Underground removal of iron and manganese. *Water Supply*, 3, 117-142.

Silvester E., Charlet L., Tournassat C., Géhin A., Grenèche J.M. and Liger E. (2005) Redox properties of FeII adsorbed onto FeIII oxy-hydroxides. *Geochim. Cosmochim. Acta* **69** (20), 4801-4815.

Singer P.C. and Stumm W. (1970) Acidic mine drainage: The rate-determining step. *Science* **167**, 1121-1123.

Søgaard E.G., Aruna R., Abraham-Peskir J. and Bender Koch C. (2001). Conditions for biological precipitation of iron by Gallionella ferruginea in a slightly polluted ground water. *Appl. Geochem*. **16**, 1129-1137.

Stipp S. L. and Hochella M. F. Jr. (1991) Structure and bonding environments at the calcite surface as observed with X-ray photoelectron spectroscopy (XPS) and low energy electron diffraction (LEED). *Geochim. Cosmochim. Acta* **55** (6), 1723-1736.

Stookey L. L. (1970) Ferrozine- A new spectrophotometric reagent for iron. *Analytical Chemistry* **42** (7), 779-81.

Stumm W. and Lee G. F. (1961) Oxygenation of ferrous iron. *Industr. Engin. Chem*. 53 (2), 143-146.

Stumm W. and Morgan J. J. (1996) Aquatic Chemistry. John Wiley & Sons, Inc. New York.

Tamura H., Goto K. and Nagayama M. (1976) The effect of ferric hydroxide on the oxygenation of ferrous ions in neutral solutions. *Corrosion Sci*. **16**, 197-207.

Tamura H., Kawamura S. and Hagayama M. (1980) Acceleration of the oxidation of Fe^{2+} ions by Fe(III)-oxyhydroxides. *Corrosion Sci*. **20**, 963-971.

Temmam M., Paquette J. and Vali H. (2000) Mn and Zn incorporation into calcite as a function of chloride aqueous concentration. *Geochim. Cosmochim. Acta* **64** (14), 2417-2430.

Teutsch N., von Gunten U., Porcelli D., Cirpka O. A., Halliday A. N. (2005) Adsorption as a cause for iron isotope fractionation in reduced groundwater. *Geochim. Cosmochim. Acta* **69** (17), 4175-4185.

USEPA (2001) Office of Water. National secondary drinking water regulations. In *Code of Federal Regulations*, 612-614.

Van Beek C. G. E. M. (1985) Experience with underground water treatment in the Netherland. *Water Supply* **3**, 1-11

Van Cappellen P., Charlet L., Stumm W. and Wersin P. (1993) A surface complexation model of the carbonate mineral-aqueous solution interface. *Geochim. Cosmochim. Acta* **57** (15), 3505-3518.

Veizer J. (1983) Trace elements and isotopes in sedimentary carbonates. In: *Carbonates: mineralogy and chemistry.* Reviews in Mineralogy Vol. 11 (ed. R. J. Reeder), Mineralogical Society of America, Washington D. C, pp. 265-299.

Von Gunten, U. and Schneider W. (1991) Primary products of the oxygenation of the iron(II) at an oxic-anoxic boundary: nucleation, aggregation and aging. *J. Colloid Interface Sci.* **145** (1), 127-139.

Wajon J. E., Ho G.-E. and Murphy P. J. (1985) Rate of precipitation of ferrous ion and formation of mixed iron-calcium carbonates by naturally occurring carbonate minerals. *Water Research* **7**, 831-837.

Wehrli B. (1990) Redox reactions of metal ions at mineral surfaces. In: *Aquatic Chemical Kinetics* (ed. W. Stumm) Wiley. New York, pp. 311-37.

Wersin P., Karthein R., Charlet L. and Stumm W. (1989) From adsorption to precipitation: sorption of Mn^{2+} on FeCO3(s). *Geochim. Cosmochim. Acta* **53** (11), 2787-2796.

WHO (2006) *Guidelines for drinking water quality*. World Health Organisation, Geneva. (http://www.who.int/water_sanitation_health/dwq/gdwq3rev/en/index.html)

Zachara J. M., Cowan C. E. and Resch C. T. (1991) Sorption of divalent metals on calcite. *Geochim. Cosmochim. Acta* **69** (20), 4801-4815.

Zachara J. M., Kittrick J. A. and Harsh J. B. (1988) The mechanism of Zn^{2+} adsorption on calcite. *Geochim. Cosmochim. Acta* **52** (9), 2281-2291.

TABLES

Table 1. Surface precipitation model parameters. > indicates a surface group; S_T = the total number of surface sites available to monolayer adsorption; X_{FeCO_3} = the mole fraction of Fe in the solid solution.

Reactions	**log K**	**Equation**
$Fe^{2+} + HCO_3^- \xleftarrow{K_a} FeCO_3(s) + H^+$	$\log K_a = -3.6$	(11)
$Ca^{2+} + HCO_3^- \xleftarrow{K_b} CaCO_3(s) + H^+$	$\log K_b = -1.849$	(12)
$Fe^{2+} + HCO_3^- + > CaCO_3^0 \xleftarrow{K_c} CaCO_3(s) + > FeCO_3^0 + H^+$	$\log K_c = 0.8$	(13)
Equations		
$S_T = [>CaCO_3^o] + [>FeCO_3^o]$		(14)
$X_{FeCO_3} = \frac{[FeCO_3(s)]}{[FeCO_3(s)] + [CaCO_3(s)]} \equiv z$		(15)
$K_a = \frac{[H^+] X_{FeCO_3}}{[Fe^{2+}][HCO_3^-]}$		(16)
$K_b = \frac{[H^+] X_{CaCO_3}}{[Ca^{2+}][HCO_3^-]}$		(17)
$K_a^{-1} K_c = \frac{[> FeCO_3^o]}{[> CaCO_3^o]} \cdot \frac{X_{CaCO_3}}{X_{FeCO_3}} \equiv B$		(18)
$TotCa = [CaCO_3(s)] + [>CaCO_3^o] + [Ca^{2+}]$		(19)
$\Gamma_{Fe} = \frac{[> FeCO_3^o]}{TotCa} + \frac{[FeCO_3(s)]}{TotCa}$		(20)
With $\frac{[> FeCO_3^o]}{TotCa} = \frac{S_T}{TotCa}(1 + B^{-1}(z^{-1} - 1))^{-1} \equiv y$		(20a)
And $\frac{[FeCO_3(s)]}{TotCa} = (z^{-1} - 1) - yB^{-1} - \frac{[H^+] \cdot z}{[HCO_3^-] \cdot K_b \cdot TotCa}$		(20b)

Table 2. Aqueous and surface speciation used to calculate fractional oxidation kinetics. > indicates calcite surface groups.

Reactions	log K	References	Eq.
$CO_2 + H_2O \leftrightarrow H^+ + HCO_3^-$	-7.82	Van Cappellen et al. (1993)	(21)
$H_2CO_3 \leftrightarrow HCO_3^- + H^+$	–6.35	Millero et al. (1995)	(22)
$HCO_3^- \leftrightarrow CO_3^{2-} + H^+$	–10.33	Millero et al. (1995)	(23)
$Fe^{2+} + HCO_3^- \leftrightarrow FeHCO_3^+$	1.47	Millero and Hawke (1992)	(24)
$Fe^{2+} + HCO_3^- \leftrightarrow FeCO_3^0 + H^+$	-4.64	Bruno et al. (1992) rev. by King	(25)
$Fe^{2+} + 2HCO_3^- \leftrightarrow Fe(CO_3)_2^{2-} + 2H^+$	–13.21	Bruno et al. (1992) rev. by King	(26)
$Fe^{2+} + HCO_3^- + OH^- \leftrightarrow Fe(CO_3)(OH)^- + H^+$	-0.36	Bruno et al. (1992) rev. by King	(27)
$Fe^{2+} + H_2O \leftrightarrow FeOH^+ + H^+$	–9.51	Millero et al. (1995)	(28)
$Fe^{2+} + 2H_2O \leftrightarrow Fe(OH)_2 + 2H^+$	–20.61	Millero et al. (1995)	(29)
$Fe^{2+} + Cl^- \leftrightarrow FeCl^+$	0.30	Pitzer (1991)	(30)
$Fe^{2+} + SO_4^{2-} \leftrightarrow FeSO_4$	2.42	Pitzer (1991)	(31)
$>CO_3H^0 \leftrightarrow >CO_3^- + H^+$	–4.9	Van Cappellen et al. (1993)	(32)
$>CO_3H^0 + Ca^{2+} \leftrightarrow >CO_3Ca^+ + H^+$	–2.8	Van Cappellen et al. (1993)	(33)
$>CO_3H^0 + Fe^{2+} \leftrightarrow >CO_3Fe^+ + H^+$	–1.6	Van Cappellen et al. (1993)	(34)
$>CO_3H^0 + FeCO_3^0 \leftrightarrow >CO_3FeCO_3H^0$	7.4	This study	(35)
$>CaOH_2^+ \leftrightarrow >CaOH^0 + H^+$	–12.2	Van Cappellen et al. (1993)	(36)
$>CaOH^0 \leftrightarrow >CaO^- + H^+$	–17.0	Van Cappellen et al. (1993)	(37)
$>CaOH^0 + HCO_3^- + H^+ \leftrightarrow >CaCO_3H^0 + H_2O$	13.8	Van Cappellen et al. (1993)	(38)
$>CaOH^0 + HCO_3^- \leftrightarrow >CaCO_3^- + H_2O$	5.2	Van Cappellen et al. (1993)	(39)

Table 3. Second order rate constants, k, (M^{-1} s^{-1}) for the reaction of Fe(II) with oxygen at 20 °C, extrapolated to I = 0 M (see text, Eq. 8). Note that King's k values were reported for 25 °C.

Reaction	**Species**	**log k I = 0**	**log k I= 0.018**	**Temperature °C**	**Reference**
(1)	$Fe^{2+} + O_2 \rightarrow Fe^{3+} + O_2^-$	–6.04	-6.21	20°	Singer and Stumm (1970)
(2)	$FeCl^+ + O_2 \rightarrow FeCl^{2+} + O_2^-$	≤ –6.04	≤-6.21	25°	King (1998)
(3)	$FeSO_4 + O_2 \rightarrow FeSO_4^+ + O_2^-$	≤–6.04	≤-6.21	25°	King (1998)
(4)	$Fe(OH)^+ + O_2 \rightarrow Fe(OH)^{2+} + O_2^-$	0.84	0.67	20°	Singer and Stumm (1970)
(5)	$Fe(OH)_2 + O_2 \rightarrow Fe(OH)_2^+ + O_2^-$	5.94	5.77	25°	King (1998)
(6)	$FeHCO_3^+ + O_2 \rightarrow FeHCO_3^{2+} + O_2^-$	<-1.53	<-1.70[a]	25°	King (1998)
(7)	$FeCO_3 + O_2 \rightarrow FeCO_3^+ + O_2^-$	<–2.53	<-2.70[a]	25°	King (1998)
(8)	$Fe(CO_3)_2^{2-} + O_2 \rightarrow Fe(CO_3)_2^- + O_2^-$	4.04	3.87	25°	King (1998)
(9)	$Fe(CO_3)(OH)^- + O_2 \rightarrow Fe(CO_3)(OH) + O_2^-$	2.22	2.05	25°	King (1998)
(10)	$>CO_3FeCO_3H^0 + O_2 \rightarrow >CO_3FeCO_3H^+ + O_2^-$	0.72 ± 0.15	0.55 ± 0.15	20°	This study

(a) For the apparent rate calculations, log k for species $FeHCO_3^+$ and $FeCO_3^o$ of -2.0 and -3.0 were used, respectively.

Table 4a. Fe(II) oxidation rate constants obtained without and with calcite (0, 1 and 10 g L^{-1}) without pre-equilibration. The added Fe(II) concentration was always 10 µM. The parameters k_{meas} and k_{app} were determined from the experimental data according to Eq. 6; k_{app} was calculated from speciation calculations and the species specific rate constants in Table 3 including the contribution by the reactive calcite surface species, $>CO_3FeCO_3H^0$.

Run N°	**Calcite**	**pH**	**O_2**	**HCO_3**	**log pCO_2**	**I**	**$[Fe(II)]_{aq}$**	**k_{meas}**	**$t_{1/2}$**	**k_{app}**	**k_{app} calculated**
	g/L		**M**	**mM**	**atm**	**M**	**M**	**s^{-1}**	**Min.**	**$M^{-1}s^{-1}$**	**$M^{-1}s^{-1}$**
No surface											
0730	none	7.04	7.6×10^{-5}	2.7	-1.81	0.018	$1.0\ 10^{-5}$	$1.0 \pm 0.1 \times 10^{-4}$	116	1.3 ±0.05	1.6
0731	none	7.06	7.6×10^{-5}	2.7	-1.85	0.018	$1.0\ 10^{-5}$	$1.35 \pm 0.03 \times 10^{-4}$	86	1.78 ±0.04	1.7
No preliminary equilibration of Fe(II) with calcite											
0626	1.01	7.08	7.8×10^{-5}	2.9	-1.8	0.018	$1.0\ 10^{-5}$	$2.75 \pm 0.1 \times 10^{-4}$	42	3.55 ±0.1	3.8
0628	1.01	7.04	8.0×10^{-5}	3.1	-1.8	0.018	$1.0\ 10^{-5}$	$2.81 \pm 0.6 \times 10^{-4}$	41	3.55 ±0.1	3.8
0630	1.01	7.03	7.5×10^{-5}	3.1	-1.8	0.018	$1.0\ 10^{-5}$	$2.83 \pm 0.4 \times 10^{-4}$	41	3.8 ±0.1	3.8
0501[b]	1.01	7.10	2.13×10^{-4}	2.6	-1.83	0.018	$1.0\ 10^{-5}$	$3.8 \pm 0.2 \times 10^{-4}$	30	1.9 ±0.2	3.8
0515[b]	1.01	7.04	2.06×10^{-4}	3.1	-1.81	0.018	$1.0\ 10^{-5}$	$3.75 \pm 0.3 \times 10^{-4}$	31	1.8 ±0.1	3.8
0601	10.1	7.05	2.13×10^{-4}	3.0	-1.8	0.018	$1.0\ 10^{-5}$	$3.4 \pm 0.3 \times 10^{-3}$	3	15.8 ±1.7	8.2 (16.0)

(b) Not used for rate calculation

Table 4b. Fe(II) oxidation rate constants obtained with calcite (1 g L^{-1}) with pre-equilibration. The added Fe(II) concentration was always 10 µM; after equilibration with calcite the remaining aqueous Fe(II) is indicated as $[Fe(II)]_{aq}$. The parameter k_{app} was determined from the experimental data according to Eq. 6; k_{app} *calculated* was determined from speciation calculation and the species specific rate constants of Table 3. In this case, it was assumed that the adsorbed calcite surface species, $>CO_3FeCO_3H^0$ did not contribute to the oxidation of Fe(II) as it was incorporated as Fe-$CaCO_3$ in the bulk solid .

After equilibration of Fe(II) with calcite

Run N°	**Calcite**	**Duration**	**pH**	**O_2**	**HCO_3**	**Log pCO_2**	**I**	**$[Fe(II)]_{aq}$**	**k_{meas}**	**$t_{1/2}$**	**k_{app}**	**$k_{app\ calculated}$**
	g/L	**hour**		**M**	**mM**	**atm**	**M**	**M**	**s^{-1}**	**Min.**	**$M^{-1}s^{-1}$**	**$M^{-1}s^{-1}$**
0720	1.01	15	7	8.0×10^{-5}	3.3	-1.73	0.018	8.3×10^{-6}	$7.0 \pm 0.3 \times 10^{-5}$	165	0.9 ±0.1	1.2
0809	1.01	15	6.99	8.0×10^{-5}	3.4	-1.71	0.018	5.6×10^{-6}	$8.8 \pm 0.3 \times 10^{-5}$	131	1.1 ±0.1	1.2
0810	1.01	15	6.95	7.4×10^{-5}	3.6	-1.7	0.018	3.5×10^{-6}	$7.1 \pm 0.4 \times 10^{-5}$	163	1.0 ±0.1	1.1
0501	1.01	168	7.06	2.13×10^{-4}	3.0	-1.80	0.018	5.2×10^{-6}	$4.5 \pm 0.4 \times 10^{-5}$	257	0.2 ±0.2	1.4
0411	1.01	168	7.05	2.1×10^{-4}	3.0	-1.80	0.018	2.0×10^{-6}	6.16×10^{-5}	188	0.3	1.4
1107[c]	1.01	24	6.95	2.0×10^{-4}	3.6	-1.65	0.018	8.7×10^{-6}	$1.27 \pm 0.4 \times 10^{-4}$	91	0.6 ±0.02	1.1
1107[c]	1.01	72	6.95	2.06×10^{-4}	3.6	-1.65	0.018	8.2×10^{-6}	$1.04 \pm 0.0 \times 20^{-4}$	111	0.5 ±0.02	1.1
1107[c]	1.01	168	7.01	2.28×10^{-4}	3.3	-1.75	0.018	6.9×10^{-6}	$1.5 \pm 0.1 \times 10^{-4}$	77	0.7 ±0.02	1.3

(c) Dried and re-suspended solid

FIGURE CAPTIONS

Figure 1

(a) First order plot of the adsorption of Fe(II) onto calcite at varying solid concentrations. **(b)** Adsorption of Fe(II) (10^{-5} M) onto 1 g L^{-1} calcite measured during 7 days. The curve corresponds to the first order kinetics determined from the slopes in (a).

Figure 2

Release of Fe(II) as function of time upon dissolution of a Fe(II) – calcite suspension purged with 20% CO_2. The suspension (1 g L^{-1}calcite) had been equilibrated with 10^{-5} M Fe(II) at pH 7.0 for 24 h (○), 72 h (◊) and 168 h (Δ) prior to the dissolution with CO_2.

Figure 3

Correlation between Fe(II) and Ca^{2+} concentrations during dissolution of calcite which was pre-equilibrated with Fe(II): 24 h (○; CO_2 20%), 48 h (◊; CO_2 100%), 168 h (Δ; CO_2 20%. ▲; CO_2 100%). The secondary X-axis, Δr, represents the estimated thickness of the dissolved calcite layer calculated from the dissolved calcium assuming a homogeneous solid composition.

Figure 4

Decrease of Fe(II) as a function of time after addition of oxygen to a Fe(II) / calcite suspension: Data measured a 1 g L^{-1} (○) and 10 g L^{-1} calcite (◊) without equilibration with Fe(II); 1 g L^{-1} calcite after 72 h equilibration with Fe(II) (●). Fe(II) 10^{-5} M, 0.20 mM O_2, pH 7.0, 4.9 mM $CaCl_2$ and 4.1 mM $NaHCO_3$.

Figure 5

Logarithmic plot of adsorption rates (closed symbols) and oxidation rates (open symbols; no prior Fe(II) - calcite equilibration) of Fe(II) in the presence of calcite. Experimental conditions: Fe(II) = 10^{-5} M, pH 7.0, 1 g L^{-1} (○) or 10 g L^{-1} calcite (◊). The oxidation experiments were carried out with 0.21 mM dissolved oxygen.

Figure 6

Adsorption isotherms of Fe(II) onto calcite measured after equilibration times of 24 hours (a), 72 hours (b) and 168 hours (c); and fit with the surface adsorption and precipitation model (SPM, solid line). The SPM assumes an adsorption (dotted line) and a co-precipitation component (dashed line) of the Fe(II) sorption. **Experimental data:** (a) 24 hours in a 1 g L^{-1} suspension, symbols ▲ and △ are duplicate runs; (b) 72 hours in a 2 g L^{-1} suspension: □; and (c) 168 hours in a 2 g L^{-1} suspension: ○.

Fits: (a, b and c) black solid line represents the fit of the 24-hour data (1 g L^{-1} calcite) obtained with the parameters log K_a = -3.6, log K_c = 0.8 and S_T = 0.98 sites nm^{-2}; (b) fit of the 72-hour data (2 g L^{-1} calcite) is shown as grey solid line, it was obtained with log K_a = -3.6; log K_c= 1.3; S_T = 1.8 sites nm^{-2}; (c) fit of the 168-hour data (2 g L^{-1} calcite) as grey solid line, log K_a = -3.6 , log K_c = 2.2, S_T = 2.5 sites nm^{-2}. K_b was

taken as the precipitation constant of calcite ($K_b = 10^{-1.85}$, Plummer and Busenberg (1982)).

Figure 7

Measured and modeled sorption of Fe(II) onto calcite, applying the parameters of the surface complexation model (SCM) and of the surface adsorption and precipitation model (SPM). For the SCM, reaction constants were taken from Van Cappellen et al. (1993; Table 2) with a surface site concentration of 5 sites nm^{-2}, respectively 3 sites nm^{-2}. For the SPM, log $K_c = 0.81$ and a surface site concentration S_T of 0.98 sites nm^{-2} were applied according to the best fit of the SPM. The triangles represent the experimental data (24-hour equilibration). The solid line represents the sum of the adsorbed Fe(II) species according to the SCM ($>CO_3Fe^+ + >CO_3FeCO_3H^0$) and the dashed line, the SCM species $>CO_3Fe^+$. The solid blue line represents the sorbed Fe(II) according to the SPM. Experimental conditions: 10^{-6} M < Fe(II) < 10^{-4} M, pH 7.0, 4.9 mM $CaCl_2$, 4.1 mM $NaHCO_3$.

Figure 8

Speciation of Fe(II) in the presence of 1 g L^{-1} calcite according to the SCM ($S_T = 3$ sites nm^{-2}) and the parameters of Table 2 with 10^{-5} M $Fe^{(II)}SO_4$, 4.9 mM $CaCl_2$ and 4.1 mM $NaHCO_3$.

Figure 9

Contribution of specific Fe(II) species to the total Fe(II) oxidation rate constant by O_2 as a function of the suspension concentration. SCM with parameters from Table 2 (S_T = 3 sites nm^{-2}); pH 7.04, calcite saturation, 4.9 mM $CaCl_2$, 4.1 mM $NaHCO_3$ and $pCO_2 = 10^{-1.79}$.

Figure 10

Contribution of specific Fe(II) species to the total Fe(II) oxidation rate by O_2 (only species that contribute > 0.01 to overall rate are shown). Calculations performed using the parameters in Table 2 and 3 for 10^{-5} M Fe(II), 4.9 mM $CaCl_2$, 4.1 mM $NaHCO_3$, 1 g L^{-1} calcite (S_T = 3 sites nm^{-2}), pH determined by the pCO_2 - calcite system.